Electronic stopping of Si from a three-dimensional charge distribution

J. Sillanpää, K. Nordlund, and J. Keinonen
Accelerator Laboratory, P.O. Box 43, FIN-00014 University of Helsinki, Finland
(Received 28 May 1999; revised manuscript received 20 March 2000)

We describe an electronic stopping model for low-energy ions, a necessity for an accurate prediction of the penetration depths of energetic ions in materials, especially in crystal channels. With the use of molecular dynamics simulations and calculating the electronic stopping from a three-dimensional charge distribution without using any free parameters, we obtain accurate range distributions on a realistic physical basis. Our electronic stopping model is based on the Brandt-Kitagawa (BK) [W. Brandt and M. Kitagawa, Phys. Rev. B **25** 5631 (1982)] theory. For heavy ions ($Z>1$) we also include a version of the Firsov inelastic energy loss model. We test our model for silicon, where plenty of experimental data are available. We first test the model for the ranges of hydrogen, to determine the accuracy of the scaling hypothesis used in the BK theory, and then for other ions. The results are compared with experimental range profiles and, with the exception of the $\langle 110 \rangle$ direction, show good agreement, comparable to that achieved with models employing free parameters. We also show that a model using an averaged electron distribution is a promising method to overcome the shortcoming in the $\langle 110 \rangle$ direction.

I. INTRODUCTION

A description of the slowing down of energetic ions penetrating matter is a long-standing problem of considerable theoretical and practical interest. Despite much intensive work during the last 80 years,[1–5] the models describing the slowing down of an ion by collisions with electrons (electronic stopping) may still give results with errors of several tens of a percent.[6–9] Ions moving in crystal channels, where the atom and electron densities are significantly below the average, present a situation that is particularly difficult. The subject is interesting not only from the theoretical but also the technological point of view, mainly because ion implantation plays an important role in semiconductor device fabrication.[10] As the size of the devices decreases, the implantation energies, annealing times, and temperatures decrease as well. At low energies the channeling of ions during the slowing down process has an important effect on the concentration profile in both the lateral and depth directions. At very low energies, implanting with tilted angles can be problematic because of shadowing effects.[11,12] Consequently the electronic stopping model used should give accurate results in channels as well as in nonchanneling directions.

Since the importance of collisions between the ion and substrate atoms (nuclear stopping) is reduced relative to the electronic stopping in crystal channels, the electronic energy loss is very important in the calculation of the ranges of channeled ions. Also, because the electron density in a channel is significantly lower than in other directions, a nonlocal electronic stopping model is not likely to work.

There have been several previous attempts to predict electronic slowing down in channels with binary collision approximation[13–16] (BCA) and molecular dynamics[15,17] (MD) programs. Unfortunately, the models have been either designed only for one ion-target combination or material or contained one or more free parameters. BCA programs also often contain nonphysical parameters (e.g., a multiple-collision parameter to account for simultaneous interactions between more than two atoms[18]) or adjust the values of some physical quantities (e.g., the Debye temperature[19]) to improve the agreement between simulated and experimental profiles.

Perhaps the best success so far has been achieved by the stopping model developed by Beardmore and Grønbech-Jensen[17] (the BGJ model). It achieves remarkable agreement between simulations and experiments by using one free parameter per ion-target pair (motivated by accounting for Z_1 oscillations[16]).

Almost all previous models use a spherically symmetric electron distribution. A few BCA models use three-dimensional (3D) charge distributions but these models are specific to one ion.[13,20] In the present paper, we combine the physically best motivated methods available for calculating stopping powers, namely, an MD treatment of the ion trajectories with electronic slowing down calculated without any free parameters from a 3D electron charge distribution. At very low energies, nuclear collisions are the dominant energy loss mechanism and any MD method can be expected to give reasonable results. To judge the quality of the model at energies where the electronic stopping dominates, we compare the results to those of the BGJ model. We also analyze the reasons for possible shortcomings of previous models and our model.

Our model contains no free parameters and can therefore be used to calculate the stopping for any ion in any target whose electron distribution can be calculated (e.g., from its structure factors[21]) without a parameter fitting process. Because the stopping is calculated from a realistic electron density, Z_2 oscillations[22] present no problem. However, in its current state the model does not take Z_1 oscillations[5] into account. Although the model is of a general nature, we first focus on silicon for which both accurate electron distributions and experimental range profiles are available in the literature.

In this paper we present ion range profiles calculated using our electronic stopping model and compare them with experimental ones measured with secondary-ion mass spectroscopy (SIMS) and nuclear resonance broadening (NRB). We concentrate on the $\langle 100 \rangle$, $\langle 110 \rangle$, and nonchanneling directions, where sufficient experimental data are available. In

Sec. II we discuss the molecular dynamics method and in Sec. III the electronic stopping model. Results for protons are presented in Sec. IV and for heavy ions in Sec. V. We discuss the results in Sec. VI and summarize them in Sec. VII.

II. MOLECULAR DYNAMICS SIMULATIONS

We used a molecular dynamics method,[23] which allows us to treat the nuclear stopping very accurately via the use of repulsive interatomic pair potentials obtained by density-functional methods.[24] This makes us confident that any differences between the simulated and experimental profiles are caused by the inaccuracy of the electronic stopping model. Unlike the BCA, the MD method is valid also at low energies. The basic algorithms of the simulation code have been discussed in detail elsewhere.[23,25,26] In short, it is an efficient MD code utilizing domain following and the recoil interaction approximation. The collisions between the ion and the target atoms are treated with pair potentials calculated with the DMol density-functional package.[27,28] The target is silicon, which has a diamond crystalline structure. The thermal displacement of atoms can have a considerable effect on channeling. We set the Debye temperature such that we get the thermal displacements measured by Buschorn *et al.*[29] The wafer temperature was assumed to be 300 K unless the source of the experimental data specified another value. We use a two-layered structure with an amorphous oxide layer on the top. At present, our code does not include any (statistical) damage model, so the ions always move in a perfect crystal. The doses used in the experiments are so low that this is a realistic approximation. If simulation of high doses is required, a damage model[30] can be incorporated easily, likewise a rare-event algorithm[17] if the tails of the range distributions are of particular interest. A beam divergence of 1°, typical of most implanters, is assumed.

III. ELECTRONIC STOPPING MODEL

A. General considerations

Our model is similar to the BGJ model,[17] except that we use a 3D instead of a spherically symmetric charge distribution and do not use any free parameters. It is also similar to the stopping model of Klein *et al.*,[31] except that we include the Firsov model for heavy ($Z_1>1$) ions, and use a 3D charge distribution and a different expression for the ionization fraction. The model is based on the Brandt-Kitagawa (BK) theory[32,4] in which electronic stopping of a heavy ion is the electronic stopping of a proton scaled by the square of the effective charge,

$$S_e = Z_{\mathrm{eff}}^2(\rho,v)S_p(\rho,v), \tag{1}$$

where ρ is the local electron density and v the velocity of the ion. Obviously, the stopping powers of protons have to be accurate. The BK theory makes several assumptions concerning, e.g., the shape of ions and does not directly take into account the quantum mechanical stopping cross section between an ion and the electrons of the target atoms. A physically more consistent way would be to calculate the heavy ion stopping directly in density-functional theory (DFT). However, a DFT-based stopping theory for all ions and targets has yet to be formulated and even the computational requirements it would pose are formidable.

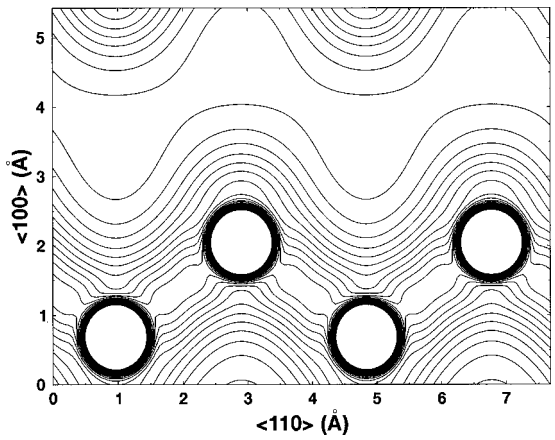

FIG. 1. Electron distribution of silicon in a (110) plane. The silicon atoms are clearly visible, as is the bond between the nearest neighbors. The contour interval is $0.05e/\text{Å}^3$ with contours going from 0.05 to 1.5. The electron density is, of course, extremely high near the nuclei.

As we calculate the stopping from a realistic local electron density, Z_2 oscillations should be reproduced. On the other hand, a source of Z_1 oscillations is not explicitly included in the model.

Atomic units will be used throughout the paper unless indicated otherwise ($e=h/2\pi=a_b=m_e=v_0=1$). The unit of stopping will therefore be 1 hartree/a_b=51.4 eV/Å, where a_b is the Bohr radius ($\approx$0.529 Å).

B. Charge distribution

The charge distribution of silicon is calculated according to the Dawson-Stewart-Coppens[21,33–35] formalism and stored in a file. We employ the Slater-type orbitals of Clementi and Roetti[36] and the fitting parameters determined by Deutsch.[21] The resulting charge distribution yields the measured structure factors.[37–39] A cross section of the charge distribution is shown in Fig. 1. In contrast to spherically symmetric charge distributions, the electron density is strongly anisotropic and

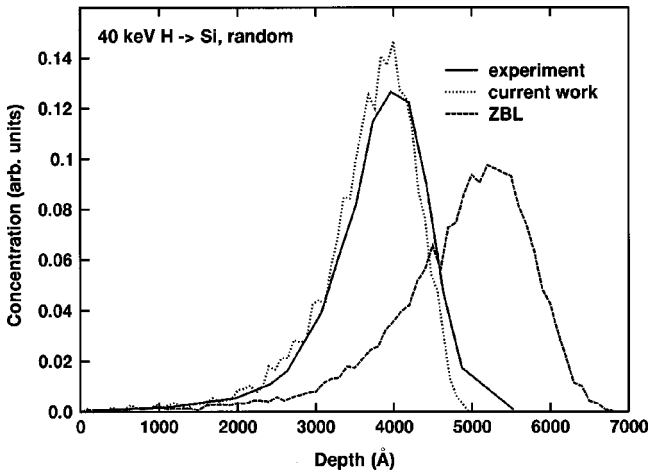

FIG. 2. Simulated and measured ranges of 40 keV protons in silicon ($\Theta=8°$, $\phi=0$). The experimental profile was measured with NRB (Ref. 49). The electronic stopping accounts for approximately 99% of the energy loss.

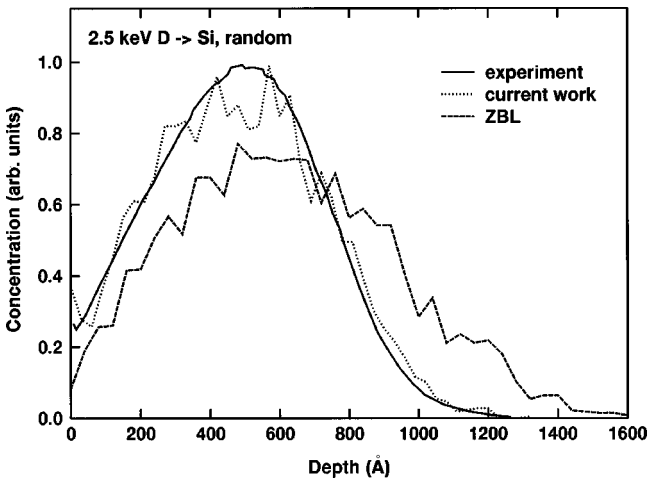

FIG. 3. Simulated and measured ranges of 2.5 keV deuterons in silicon ($\Theta = 11°$). The experimental profile was measured with SIMS (Ref. 50). The electronic stopping accounts for approximately 76% of the energy loss.

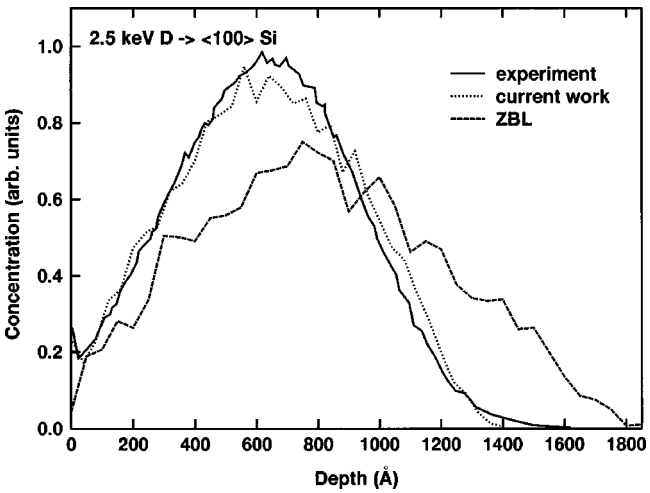

FIG. 4. Simulated and measured ranges of 2.5 keV deuterons in the $\langle 100 \rangle$ channel of silicon. The experimental profile was measured with SIMS (Ref. 50). The electronic stopping accounts for approximately 80% of the energy loss.

the bond between the nearest neighbors is clearly discernible. We used the fit obtained by Deutsch for convenience only; the charge distribution can also be obtained from a set of sufficiently accurate structure factors by an inverse Fourier transform[40,41] or calculated by *ab initio* methods.[42] During the simulations the local electron density is interpolated from a precalculated 3D table.

C. Protons

For velocities below the Fermi velocity v_0, the nonlinear density-functional calculations of Puska *et al.*[43,44] give the stopping of a proton as

$$S_{\mathrm{Ech}} = \frac{3v}{k_F r_s^3} \sum_{l=0}^{\infty} (l+1) \sin^2[\delta_l(E_F) - \delta_{l+1}(E_F)], \qquad (2)$$

where $\delta_l(E_F)$ is the phase shift for the scattering of an electron at the Fermi energy, the one-electron radius $r_s = [3/(4\pi\rho)]^{1/3}$, and k_f the Fermi momentum. Because this is very time consuming to calculate, the stopping of protons is calculated from linear response theory and multiplied by a correction factor[15] to obtain the result of Echenique *et al.* The Firsov model is not used in the calculation of the stopping for protons because it would lead to a much too strong stopping. This is not suprising, since the validity of Firsov's original formulation[45,46] is limited to cases where $0.25 \leqslant Z_1/Z_2 \leqslant 4$, and although later formulations[47,48] have tried to overcome this limitation, they still work best when $Z_1 \approx Z_2$. If one wants to simulate high-energy implantation, another expression for the stopping of protons can be inserted into the model.

D. Heavy ions

To obtain the electronic stopping of a heavy ion we calculate its effective charge using the formulas in Ref. 5. We do not use any free parameters but rather calculate it from the local one-electron radius r_s. For brevity, only one equation is subjected to closer examination, namely, the one that gives the ionization fraction q (the number of electrons in an ion divided by its Z) as a function of the reduced relative velocity y_r,

$$q = 1 - e^{-0.95(y_r - 0.07)}. \qquad (3)$$

Equation (3) is taken from Ref. 5 and was also used in Ref. 15. It is a fit to experimental data. Ziegler *et al.*[5] note that because of lack of experimental data at low energies it should not be used if $y_r < 0.10$. If $y_r < 0.07$, it will give negative q values, meaning that the ion will gain electrons. Of the ions simulated here, this situation can arise with arsenic and indium at low charge densities and with phosphorus at extremely low charge densities but not with boron. The value of the charge density, where the ionization fraction goes negative, decreases slightly with increasing velocity (for 2 keV As this occurs at $r_s \approx 1.06$ Å and for 100 keV As at

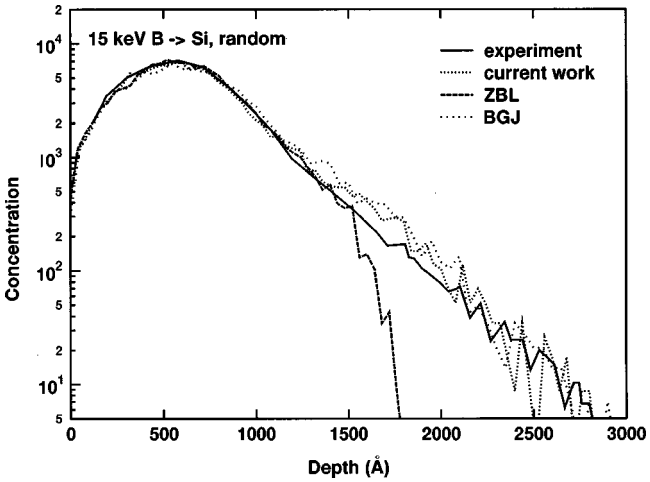

FIG. 5. Simulated and measured ranges of 15 keV B ions in silicon ($\Theta = 7°$, $\phi = 30°$). The experimental range profile was measured with SIMS (Ref. 17). The nuclear stopping accounts for approximately 50% of the energy loss and the electronic stopping for 50% (of which the Firsov model accounts for 22 percentage points).

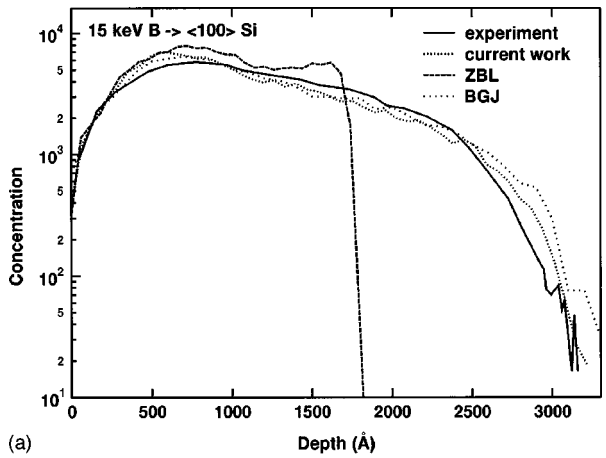

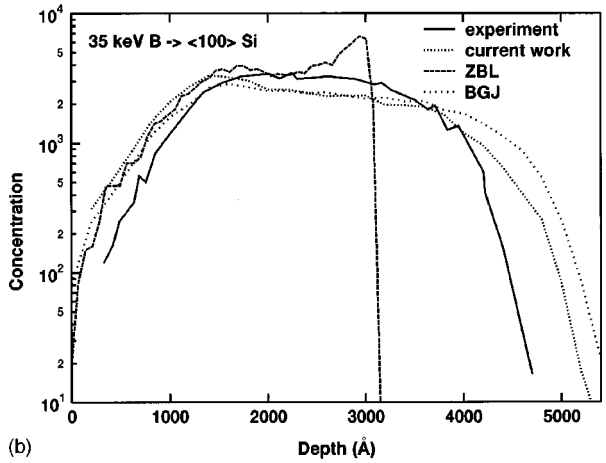

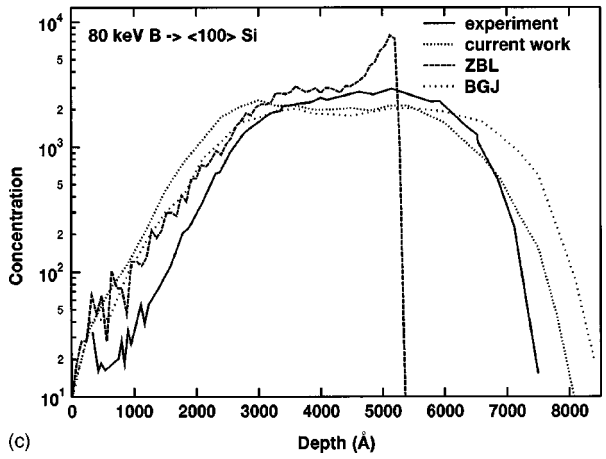

FIG. 6. Simulated and measured ranges of B ions in the ⟨100⟩ channel of silicon. The experimental profiles were measured with SIMS (Ref. 15). In (a), the nuclear stopping accounts for approximately 37% and the electronic stopping for 63% [of which the Firsov model accounts for 27 percentage points (pp)] of the energy loss. In (b), the percentages are 21% and 78% (33 pp) and in (c) 12% and 89% (37 pp), respectively.

$r_s \approx 1.125$ Å). The stopping will still be positive because it is proportional to the square of the effective charge. We made some simulations using the expression for ionization fraction given by Klein *et al.*,[31] which is always positive, but the difference in the results was negligible. An expression good also for low velocities is still desirable, but since the

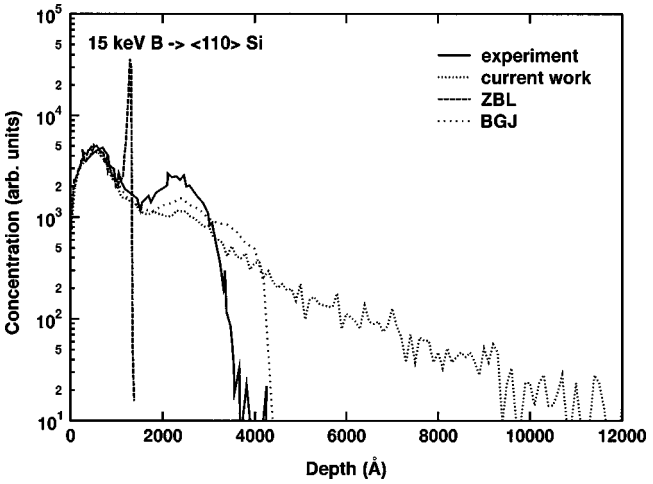

FIG. 7. Simulated and measured (Ref. 15) ranges of 15 keV B ions in the ⟨110⟩ channel of silicon. The nuclear stopping accounts for approximately 30% of the energy loss and the electronic stopping 70% (of which the Firsov model accounts for 26 percentage points).

main objective of the present work is testing a 3D charge distribution within existing models, we have not sought another fit.

We include the Firsov model to describe the energy loss due to inelastic collisions with target atoms by using the approach derived by Elteckov *et al.*,[48] where the slowing force (in Newtons) is given by

$$F(R,v) = \frac{-0.7h}{(\pi a_b)^2}\left(\frac{Z_A^2}{(1+0.8\alpha Z_A^{1/3}R/a_B)^4} + \frac{Z_B^2}{[1+0.8(1-\alpha)Z_B^{1/3}R/a_B]^4}\right) v \text{ N}, \qquad (4)$$

where Z_A and Z_B $(Z_A > Z_B)$ are the atomic numbers, a_B the Bohr radius, R the interatomic distance, and $\alpha = 1/[1 + (Z_B/Z_A)^{1/6}]$.

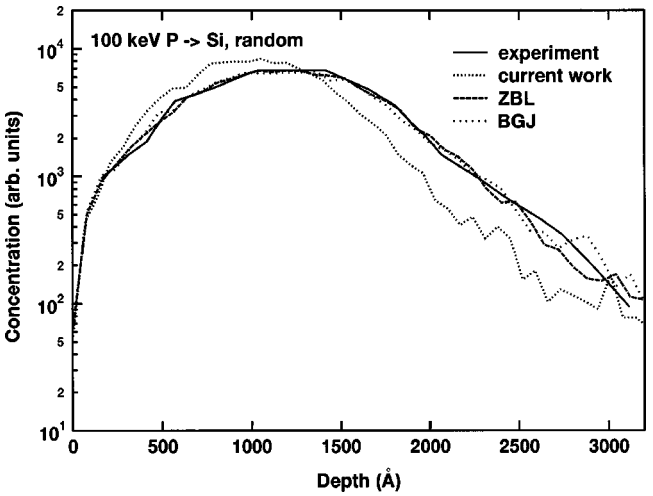

FIG. 8. Simulated and measured ranges of P ions in silicon, $(\Theta = 10°,\ \phi = 15°)$. The experimental range profiles were measured with SIMS. (Ref. 16) The nuclear stopping accounts for 58% of the energy loss and the electronic stopping for 43% (of which the Firsov model accounts for 15 percentage points).

IV. RANGE DISTRIBUTIONS OF PROTONS

Before trying to calculate the stopping for heavy ions, we had to check the accuracy of the electronic stopping for protons. Range profiles obtained with our model are compared with those observed experimentally and those obtained with the Ziegler-Biersack-Littmark (ZBL) model. Figure 2 shows that our stopping model results in a clear improvement over the ZBL model. In all figures the depth profiles have been normalized so that the areas under them are equal.

We also simulated the ranges of 2.5 keV deuterons[50] in several directions, Figs. 3 and 4. The agreement between the simulations and experimental data is good. We are confident in using scaling to obtain the stopping of heavy ions. A combination of the BK theory and Firsov model was also tested but gave much too strong stopping powers. We also tried to reproduce the elastic recoil detection (ERD) data of Bourque and Terreault,[51] but did not achieve good agreement. The maxima of the simulated profiles were some 200 Å deeper in all directions, including the nonchanneling directions where our model shows good agreement with other experiments. The reason for the discrepancy is assumed to be the uncertainty in the location of the target surface in the ERD profiles.

V. RANGE DISTRIBUTIONS OF HEAVY IONS

Our model can be used to calculate the electronic stopping for any ion. We chose arsenic, boron, phosphorus, and indium because they are commonly used dopants and sufficient as-implanted experimental range data exist to test the accuracy of our simulations. We ran simulations for various cases including the data for these ions found in Refs. 11–17, 31, 52 and 46. For brevity, only some representative cases for each ion will be shown. The version of the BGJ model used for comparison uses Eq. (4) for the Firsov model and the same interatomic potentials as other models shown here. We also tried to simulate the ranges of Al in silicon but predicted a much too strong stopping. The BGJ model has similar difficulties with aluminum.[17]

A. Boron

We achieve good agreement in nonchanneling and ⟨100⟩ directions, Figs. 5 and 6. In these directions our model is at least as accurate as the BGJ model. The ZBL stopping performs fairly well in nonchanneling directions but overestimates the stopping in channels. Because the ZBL stopping is a nonlocal parametrization, its use in channels also leads to range profiles with unrealistically sharp end of ranges.

In the ⟨110⟩ direction the agreement is not very good; see Fig. 7. In this case, the experimental profile consists of two peaks, one corresponding to the nonchanneled ions and the other to channeled ions. We predict the first of these two correctly, but predict too long ranges for the channeled ions. The most likely explanation is that because the effective charge is calculated from the electron density at the center of the ion,[31] we calculate it from the extremely low electron density at the center of the channel. To take the finite size of the ion into account, an averaging procedure might be useful. We will explore this possibility in Sec. VI.

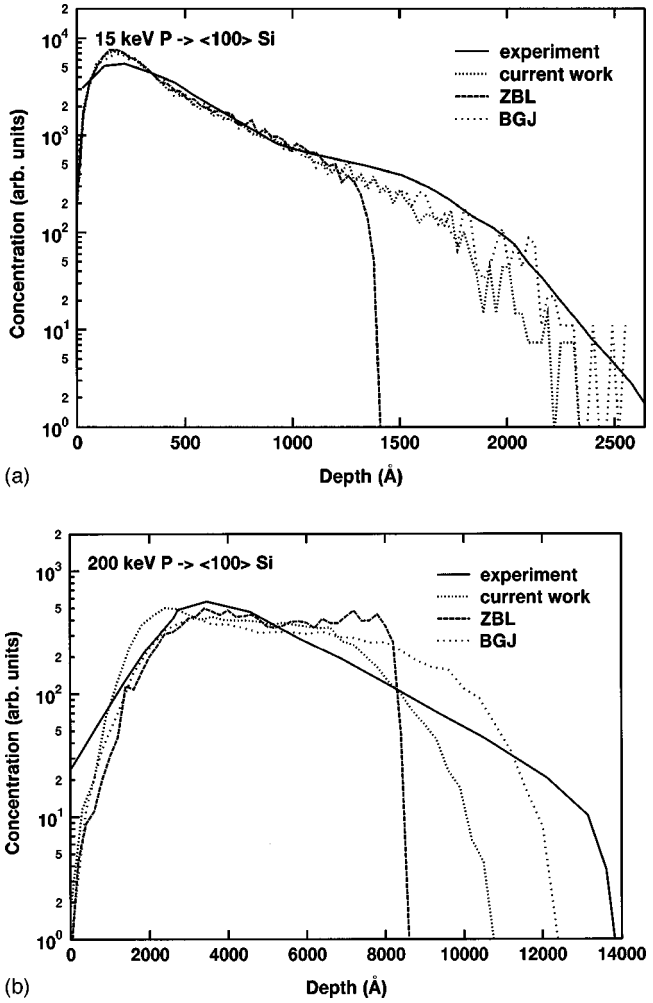

FIG. 9. Simulated and measured (Ref. 16) ranges of P ions in the ⟨100⟩ channel of silicon. In (a), the nuclear stopping accounts for 70% of the energy loss and the electronic stopping for 30% (of which the Firsov model accounts for 10 percentage points). In (b), the percentages are 22% and 78% (27 pp), respectively

B. Phosphorus

As can be seen in Figs. 8 and 9, reasonable agreement is achieved for both nonchanneling and ⟨100⟩ data. In the ⟨110⟩ direction, not shown here, the results were similar to those obtained for boron. Our model does not perform as well as the BGJ stopping: the peaks of the simulated profiles are too close to the surface also in random directions, indicating a need to adjust the model for Z_1 oscillation. The ZBL stopping works well in nonchanneling directions but fails in channels.

C. Arsenic

Reasonable agreement is achieved also for arsenic, Figs. 10 and 11. The exception is the ⟨110⟩ channel were we overestimate the ranges. As before, the ZBL electronic stopping is sufficiently accurate in nonchanneling directions but overestimates the stopping in the channels.

D. Indium

The measured and simulated indium profiles, shown in Fig. 12, are also in good agreement, the tail of the calculated

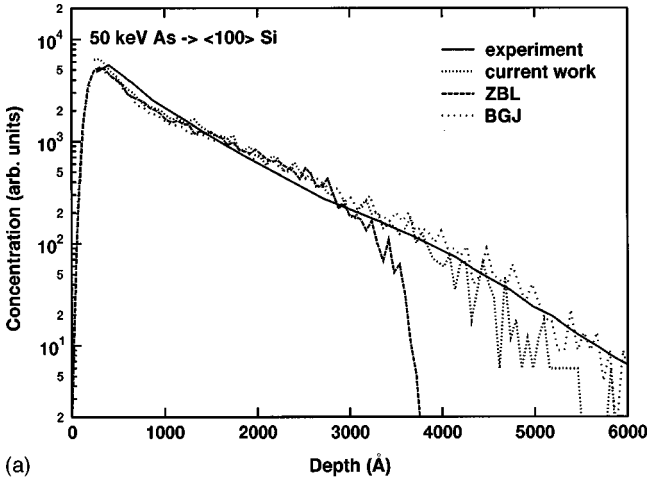

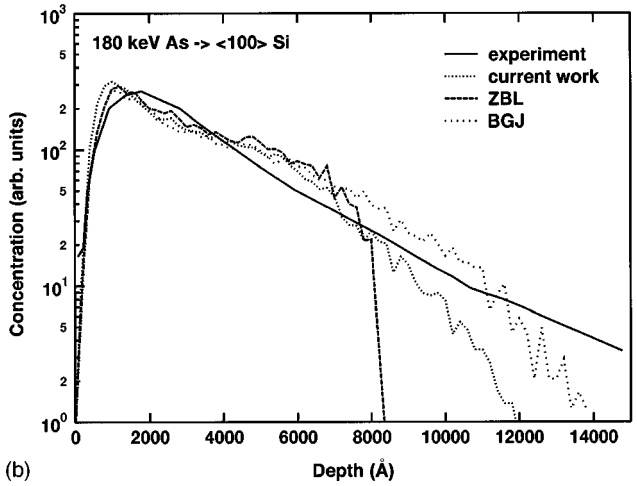

FIG. 10. Simulated and measured ranges of As ions in the ⟨100⟩ channel of silicon. The experimental range profiles were measured with SIMS (Ref. 15). In (a), the nuclear stopping accounts for approximately 68% of the energy loss and the electronic stopping for 32% (of which the Firsov model accounts for 12 percentage points). In (b), the percentages are 45% and 54% (21 pp), respectively

range profile having a slightly weaker intensity. We do not present any data for the BGJ model because we do not have a value for the one-electron radius. No experimental data was found for the ⟨110⟩ channel.

VI. DISCUSSION

The accuracy of the electronic stopping for protons is good, clearly better than that of the ZBL stopping, even in non-channeling directions. The results are sufficiently accurate so that the electronic stopping of a heavy ion can be calculated by scaling the stopping of protons.

For heavy ions, the model predicts the electronic stopping quite accurately in ⟨100⟩ and nonchanneling directions but runs into trouble in the ⟨110⟩ channel. Two possible reasons for this are (1) the use of a charge distribution of a perfect crystal without thermal displacements and (2) the use of the electron density at the center of the ion in the calculation of the effective charge. We tested the former assumption (1) by simulating the ranges of arsenic ions in the ⟨110⟩ channel using our charge distribution and the stopping model of

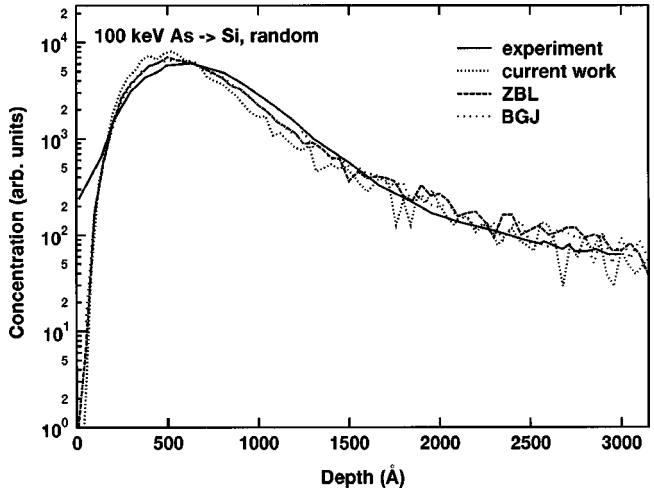

FIG. 11. Simulated and measured ranges of 100 keV As ions in silicon ($\Theta = 8°$, $\phi = 30°$). The experimental range profile was measured with SIMS (Ref. 17). The nuclear stopping accounts for approximately 75% and the electronic stopping for 25% (of which the Firsov model accounts for 8 percentage points) of the energy loss. The figure is cut off at 3300 Å because there is no experimental data beyond 3000 Å.

Yang *et al.*[13] This stopping model is accurate for As implants but unfortunately untransferable for other ions. As the agreement between simulated and experimental range profiles was better than with our model, we conclude that the absence of thermal displacements in the charge distribution is not likely to play a major role at room temperature.

Testing the latter assumption (2) is slightly more complicated. The finite size of the atoms could be dealt with by not using the value of electron density at the center of the ion but rather by taking an average of the charge distribution. Taking the size of the ion into consideration is also necessary if one wants to account for Z_1 oscillations. We need to do this because we did not get a satisfactory agreement for aluminum in any direction (this ion-target combination presents problems for other models as well[17]). However, we know of no attempt to do this in the low-velocity regime. To test to what extent an averaging scheme improves agreement in channels, we averaged the charge distribution over a spherical region of radius r. As the averaging radius is increased, ⟨100⟩ channels close first, followed by the ⟨110⟩ channels; see Fig. 13. There is only a very small effect in nonchanneling directions.

Of course, we need a physical motivation for the averaging radius. Otherwise we just end up with another free parameter and there already is a one-parameter model that works well, the BGJ model. However, the simple scheme used here is sufficient to demonstrate that much, if not most, of the remaining problems of stopping in channels can be dealt with by an averaging scheme. The results presented here were not very sensitive to the value of the radius. To take the Z_1 oscillations properly into account a more realistic treatment of the electron structure of the ion, instead of the exponential decay used in the BK theory, should be introduced. There is also the question of finding a better expression for the ionization fraction. We intend to address these matters in the near future.

To gauge the advantages of using a 3D distribution we also ran some simulations using our model and a spherically

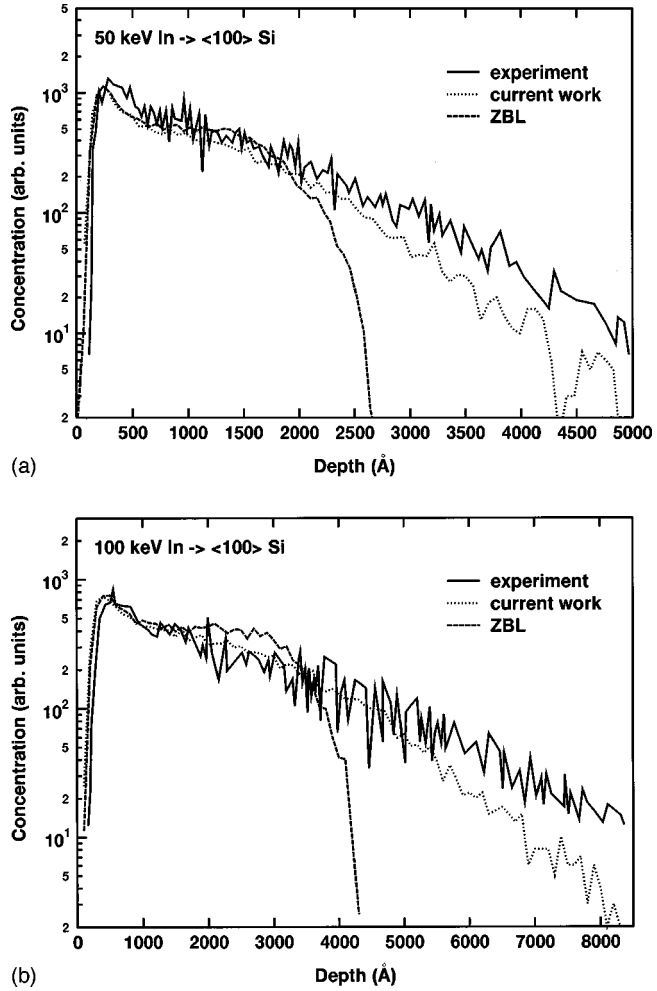

FIG. 12. Simulated and measured ranges of In ions in the ⟨100⟩ channel of silicon. The experimental range profiles were measured with SIMS (Ref. 53). In (a), the nuclear stopping accounts for 71% and the electronic stopping for 29% (of which the Firsov model accounts for 13 percentage points) of the energy loss. In (b), the percentages are 63% and 36% (16 pp), respectively.

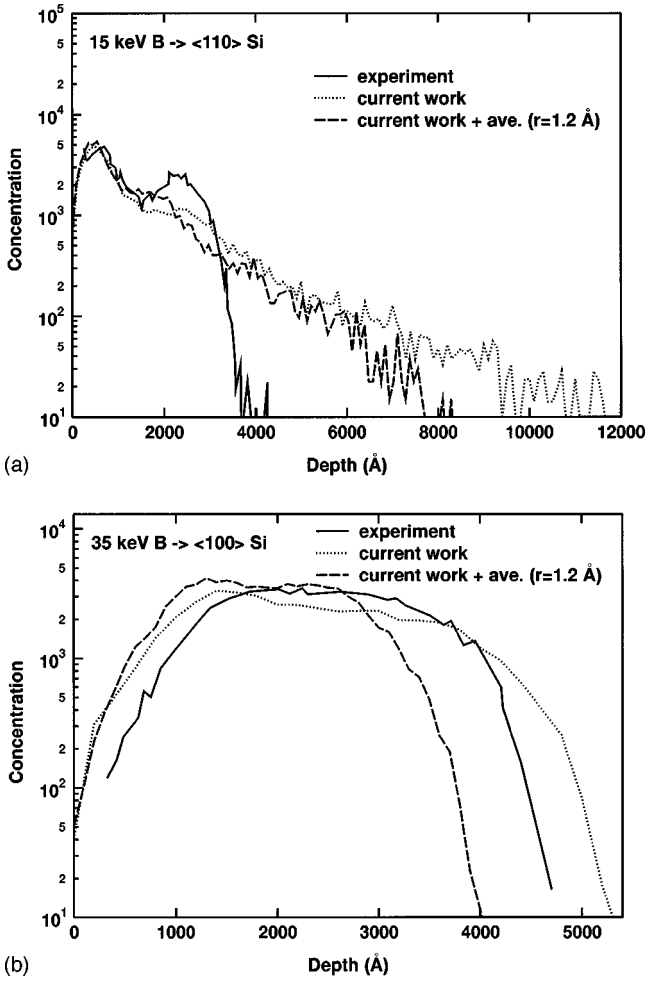

FIG. 13. Effect of taking an average of the charge distribution when calculating heavy ion stopping. The results are not very sensitive to the value of the averaging radius.

symmetric charge distribution[5] used, e.g., in the BGJ model. As can be seen in Fig. 14, the difference in charge distributions does show in the range profiles.

The agreement between the simulated and experimental profiles is generally slightly better at lower energies, which are also more interesting from the technological point of view. This is mostly due to the fact that the nuclear stopping, which the MD method takes into account very accurately, is more important there. Even at higher energies, where the electronic energy loss dominates, the agreement does not get markedly worse. Our equation for the stopping of protons assumes that the velocity of the ion is small compared to the Bohr velocity. This assumption, which is inherent in all models using the Echenique stopping for protons,[14–17,43] and the resulting velocity-proportional stopping begin to break down at high energies.

VII. CONCLUSIONS

We have developed a local electronic stopping model with no free parameters. It can be used to calculate the electronic stopping for any ion in any target whose electron density distribution can be acquired. As a first test of this model, we implemented it into an MD method and used it to calculate as-implanted range profiles in crystalline silicon. For hydrogen, the agreement between simulated and measured profiles is good. For the heavy ions examined, the agreement with experimental profiles is good in nonchanneling direc-

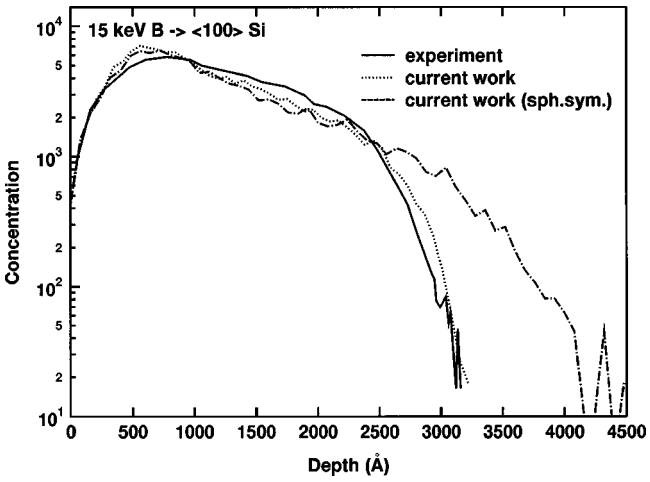

FIG. 14. Effect of the charge distribution on the range profiles.

tions and ⟨100⟩ crystal channels but not very good in the ⟨110⟩ channels known to be difficult to handle accurately. Our simulations show that a major reason for this is the unrealistic treatment of the ion as pointlike when calculating the effective charge. Nevertheless, the results obtained in this study show that the use of realistic 3D electronic charge distributions provides good grounds for accurate and transferable electronic slowing down models.

ACKNOWLEDGMENTS

We wish to thank Professor. M. Deutsch for his help with calculating the charge distribution. The research was supported by the Academy of Finland under Project Nos. 35073 and 44215. Grants of computer time from the Center for Scientific Computing in Espoo, Finland are gratefully acknowledged.

[1] N. Bohr, Philos. Mag. **25**, 10 (1913).
[2] H.A. Bethe, Ann. Phys. (Leipzig) **5**, 325 (1930).
[3] E. Fermi, Phys. Rev. **57**, 485 (1940).
[4] W. Brandt and M. Kitagawa, Phys. Rev. B **25**, 5631 (1982).
[5] J. F. Ziegler, J. P. Biersack, and U. Littmark, *The Stopping and Range of Ions in Matter* (Pergamon, New York, 1985).
[6] P. Haussalo, K. Nordlund, and J. Keinonen, Nucl. Instrum. Methods Phys. Res. B **111**, 1 (1996).
[7] J. Sillanpää, E. Vainonen-Ahlgren, P. Haussalo, and J. Keinonen, Nucl. Instrum. Methods Phys. Res. B **142**, 1 (1998).
[8] J. Keinonen, K. Arstila, and P. Tikkanen, Appl. Phys. Lett. **60**, 228 (1992).
[9] K. Arstila, J. Keinonen, and P. Tikkanen, Nucl. Instrum. Methods Phys. Res. B **101**, 321 (1995).
[10] *Handbook of Ion Implantation Technology*, edited by J. F. Ziegler (North-Holland, New York, 1992).
[11] D. Downey, C. Osburn, and S. Marcus, Solid State Technol. **40** (12), 71 (1997).
[12] V. Raineri, R.J. Schreutelkamp, F.W. Saris, R.E. Kaim, and K.T.F. Janssen, Nucl. Instrum. Methods Phys. Res. B **59/60**, 1056 (1991).
[13] S. Yang, S.J. Morris, S. Tian, K.B. Parab, and A.F. Tasch, IEEE Trans. Semicond. Manuf. **9**, 49 (1996).
[14] K.M. Klein, C. Park, and A.F. Tasch, IEEE Trans. Electron Devices **39**, 1614 (1992).
[15] D. Cai, N. Grønbech-Jensen, C.M. Snell, and K.M. Beardmore, Phys. Rev. B **54**, 17 147 (1996).
[16] D. Cai, C.M. Snell, K.M. Beardmore, and N. Grønbech-Jensen, Int. J. Mod. Phys. C **9**, 459 (1998).
[17] K.M. Beardmore and N. Grønbech-Jensen, Phys. Rev. E **57**, 7278 (1998).
[18] M.T. Robinson and I.M. Torrens, Phys. Rev. B **9**, 5008 (1974).
[19] G. Hobler, A. Simionescu, L. Palmetshofer, F. Jahnel, R. von Criegern, C. Tian, and G. Stingeder, J. Vac. Sci. Technol. B **14**, 272 (1996).
[20] E. Morvan, P. Godignon, S. Berberich, M. Vellvehi, and J. Millan, Nucl. Instrum. Methods Phys. Res. B **147**, 68 (1999).
[21] M. Deutsch, Phys. Rev. B **45**, 646 (1992); **46**, 607 (1992).
[22] W. Brandt, Nucl. Instrum. Methods Phys. Res. **194**, 13 (1982).
[23] K. Nordlund, Comput. Mater. Sci. **3**, 448 (1995).
[24] K. Nordlund, N. Runeberg, and D. Sundholm, Nucl. Instrum. Methods Phys. Res. B **132**, 45 (1997).
[25] J. Keinonen, A. Kuronen, K. Nordlund, R.M. Nieminen, and A.P. Seitsonen, Nucl. Instrum. Methods Phys. Res. B **88**, 382 (1994).
[26] K. Nordlund and A. Kuronen, Nucl. Instrum. Methods Phys. Res. B **115**, 528 (1996).
[27] J. Delley, J. Chem. Phys. **92**, 508 (1990).
[28] DMol is a trademark of Bio Sym. Inc., San Diego, CA.
[29] G. Buschorn, E. Diedrich, W. Kufner, M. Rzepka, H. Genz, P. Hoffman-Stascheck, and A. Richter, Phys. Rev. B **55**, 6196 (1997).
[30] H.J. Kang, R. Shimizu, T. Saito, and H. Yamakawa, J. Appl. Phys. **62**, 2733 (1987).
[31] K.M. Klein, C. Park, and A.F. Tasch, Appl. Phys. Lett. **57**, 2701 (1990).
[32] A. Mann and W. Brandt, Phys. Rev. B **24**, 4999 (1981).
[33] B. Dawson, Proc. R. Soc. London, Ser. A **298**, 379 (1967).
[34] R.F. Stewart, J. Chem. Phys. **58**, 1668 (1973).
[35] N.K. Hansen and P. Coppens, Acta Crystallogr., Sect. A: Cryst. Phys., Diffr., Theor. Gen. Crystallogr. **34**, 909 (1978).
[36] E. Clementi and C. Roetti, At. Data Nucl. Data Tables **14**, 177 (1974).
[37] P.J.E. Aldred and M. Hart, Proc. R. Soc. London, Ser. A **332**, 223 (1973); **332**, 239 (1973).
[38] S. Cummings and M. Hart, Aust. J. Phys. **41**, 423 (1988).
[39] R. Teworte and U. Bonse, Phys. Rev. B **29**, 2102 (1984).
[40] Z.W. Lu, A. Zunger, and M. Deutsch, Phys. Rev. B **47**, 9385 (1993).
[41] M. Deutsch and M. Hart, Phys. Rev. B **31**, 3846 (1985).
[42] J.M. Zuo, P. Blaha, and K. Schwarz, J. Phys.: Condens. Matter **9**, 7541 (1997).
[43] P.M. Echenique, R.M. Nieminen, and R.H. Ritchie, Solid State Commun. **37**, 779 (1981); M. J. Puska and R. M. Nieminen, Phys. Rev. B **27**, 6121 (1983).
[44] P.M. Echenique, R.M. Nieminen, J.C. Ashley, and R.H. Ritchie, Phys. Rev. A **33**, 897 (1986).
[45] O.B. Firsov, Zh. Éksp. Teor. Fiz. **36**, 1517 (1959) [Sov. Phys. JETP **36**, 1077 (1959)].
[46] C.S. Murthy and G.R. Srinivasan, IEEE Trans. Electron Devices **39**, 264 (1992).
[47] L. Kishinevskii, Bull. Acad. Sci. USSR, Phys. Ser. **26**, 1433 (1962).
[48] V. A. Elteckov, D. S. Karpuzov, Y. V. Martynenko, and V. E. Yurasova, in *Atomic Collision Phenomena in Solids*, edited by D. Palmer, M. W. Thompson, and P. D. Townsend (North-Holland, Amsterdam, 1970), p. 657.
[49] P. Torri, J. Keinonen, and K. Nordlund, Nucl. Instrum. Methods Phys. Res. B **84**, 105 (1994).
[50] C.W. Magee, S.A. Cohen, D.E. Voss, and D.K. Brice, Nucl. Instrum. Methods **168**, 383 (1980).
[51] G. Bourque and B. Terreault, Nucl. Instrum. Methods Phys. Res. B **140**, 13 (1998).
[52] R. Wilson, J. Appl. Phys. **60**, 2797 (1986).
[53] Y. Chen, B. Obradovic, M. Morris, G. Wang, G. Balamurugan, D. Li, A. F. Tasch, D. Kamenitsa, W. McCoy, S. Baumann, R. Bleier, D. Sieloff, D. Dyer, and P. Zeitzoff, J. Tech. Comput. Aided Design (1999).